Journal of Physics D: Applied Physics 50 (2017) 155002 (5pp),

doi: 10.1088/1361-6463/aa5b1c

Universal Scaling of the Anomalous Hall Effect

Xiaoqian Zhang,[1,b)] Wei Wang,[1,b)] Kejie Wang,[1] Wei Niu,[1] Bolin Lai,[1] Nick Maltby,[2] Mao Yang,[1] Ming Gao,[1] Wenqing Liu,[2] Liang He,[1,a)] Rong Zhang,[1] Yongbing Xu[1,2,a)]

[1] *Jiangsu Provincial Key Laboratory of Advanced Photonic and Electronic Materials, Collaborative Innovation Center of Advanced Microstructures, School of Electronic Science and Engineering, Nanjing University, Nanjing 210093, China*

[2] *York-Nanjing Joint Centre (YNJC) for spintronics and nano engineering, Department of Electronics, The University of York, YO10 3DD, United Kingdom*

ABTRACT

We have undertaken a detailed study of the magneto-transport properties of ultra-thin Fe films epitaxially grown on GaAs(100). A metal-semiconductor transition has been observed with a critical thickness of 1.25 nm, which was thought to be related to the thermally activated tunneling between metallic clusters. By fitting ρ_{AH} versus ρ_{xx}^2 with TYJ equation,[1] we found the magnetization is negligible for the scaling of the anomalous Hall effect in ultra-thin Fe film. Furthermore, the intrinsic term which is gotten by linear fitting of ρ_{AH} versus ρ_{xx}^2 shew an obvious decrease with the film thickness dropped below 1.25 nm, which was thought to be related to the fading of the Berry curvature in the ultra-thin film limit.

The behaviors of magnetic thin films grown on semiconductor substrates gain growing interests due in part to the potential applications of spin-sensitive heterostructure devices.[2, 3] Fe films grown on GaAs substrates have been widely studied, for their high Curie temperature and small lattice mismatch between bcc Fe and GaAs.[4-6] For magnetic materials, the anomalous Hall effect (AHE) is one of the most significant phenomena. However, for more than five decades, its physical microscopic mechanism remains controversial. At the same time, the influence of the changing thickness on the magnetization of ultra-thin ferromagnetic films is a considerable interesting topic.

The transport properties of the Fe/GaAs system has been studied by Xiaofeng Jin *et al*., by whom a comprehensive scaling between the anomalous Hall conductivity (AHC) and longitudinal conductivity has been established. It is very clear that the AHE involves three main mechanisms: skew scattering, side jump and Berry curvature. Especially at high temperature, the Berry curvature contribution dominates. [7-9] However, the electronic properties of Fe films below 1.5 nm on GaAs substrate are poorly explored, and this is the starting point of our work.

In this work, we explore the structural and magneto-transport properties of the ultra-thin Fe films ranging from 0.53 nm to 17 nm. A metal-semiconductor transition has been observed, in this system with a critical thickness of 1.25 nm. For the anomalous Hall resistivity ρ_{AH} of film thickness below 1.25 nm, an obvious departure from the linear relationship appears at high temperature. And we attribute it to the reduction of the magnetization. The intrinsic anomalous Hall conductivity (AHC) was extracted, and we found it decreases when film thickness decreasing below 1.25 nm. It indicates that the size effect can change the Berry curvature contribution for Fe films grown on GaAs (100).

To prepare the samples, we used highly insulating GaAs (100) epi-ready wafers, and the Fe thin films were grown in an ultra high vacuum MBE system with the pressure below 3×10^{-9} mbar. Before the growth, GaAs (100) substrates were annealed at 580 ºC to remove Gallium oxide, monitored by the in-situ reflection high energy electron diffraction (RHEED). High purity Fe (99.999%) was evaporated with the substrates sitting at room temperature. The as-grown Fe film demonstrated atomic flat surface as evidenced by streaky RHEED patterns (Fig. 1**a**). The deposition rate of ~ 1 ML per min was measured by a quartz microbalance, which was calibrated by thickness measurements using atomic force microscopy. After the growth, Fe thin films were capped with a 2 nm-thick Cr layer to prevent oxidation in air. Fig. 1b exhibits a large-scale atomic force microscope (AFM) image of an as-grown 2.45 nm Fe film with Cr capping layer. The root mean square (RMS) is 0.16 nm, indicating that the surface is very smooth.

Magnetization hysteresis loops for different Fe thicknesses measured by VSM at room

temperature are shown in Fig. 1**c**, with the magnetic field applied along GaAs [110] direction. The saturation magnetic moment increases as film thickness increases. Fig. 1**c** inset exhibits the thickness dependent saturation magnetization per cm^2 for a set of samples. The slope (M_0 = 0.141×10^4 emu/cm^3) extracted from the linear fitting (blue line in Fig. 1c bottom inset) is close to the bulk Fe value, suggesting the high quality of our samples.[10] The error bars not shown are comparable with the size of the data symbols. We have also noticed a non-zero intercept of 0.7 nm (about 5 ML) at the horizontal axis, which has been described as a magnetically "dead layer" at the interface. And this number is consistent with previous report on Fe films grown on S-passivated GaAs substrates, which is ~ 4.8 ML.[11] The excellent quality of the Fe(6.3 nm)/GaAs(100) heterostructures is demonstrated by cross-sectional high-resolution transmission electron microscopy (HRTEM), shown in Fig. 1c top inset, from which an atomic sharp interface can be seen.

To explore the transport properties of the heterostructures, samples were cut into 2 × 8 mm^2 pieces, then standard six-contact Hall bar geometry were adopted to do the transport measurements. The longitudinal resistance R_{xx} and the transverse resistance R_{xy} were measured in a Quantum Design physical properties measurement system (PPMS-9T). Keithley 6221 provided AC current source of 1 mA with a frequency of 17 Hz, and SR830 Lock-in Amplifiers detected the corresponding voltage signals. The temperature ranged from 2 to 400 K with the highest magnetic field up to 9 T perpendicular to the surfaces.[12]

As plotted in Fig. 2**a**, the temperature-dependent sheet resistances (R_s) of the Fe films exhibit a metal-semiconductor transition at a critic thickness of 1.25 nm (9 ML). Above it, the thicker films show classical metallic behavior with a positive slope as a function of temperature, which originates from the phonon scattering. Below it, the resistances increase as the temperatures decrease. This semiconductive behavior for thinner films is probably caused by Fe nanoclusters. In the ultrathin film regime, which is below the coalescence threshold, Fe forms three dimensional single crystal clusters with an average diameter of a few nanometers on GaAs. The observed semiconductive behavior is a strong indication that the main mechanism for electron conduction is thermally activated tunneling between metallic clusters.

The thickness dependent sheet resistance (R_s) and carrier density (N_{2D}) are plotted in Fig. 2**b** & 2**c**, respectively. At 10 K, R_s demonstrates a monotonic increase as film thickness decreases, especially for thickness below 1.25 nm, the trend becomes much sharper. For R_s is supposed to be proportional to 1/d (d representing the film thickness), the result in Fig. 2**b** makes sense. Accordingly in Fig. 2**c**, the 2D carrier density decreases, and saturates to a constant value of $\sim1\times10^{15}cm^{-2}$ below 1.25 nm, which we believe is the carrier density of the Fe nanoclusters.

Based on this finding, we try to complete a comprehensive understanding of the scaling of the anomalous Hall effect. The thickness of Fe films for the transport measurements is pushed to a limit of 0.53 nm (4 ML) in this work. The semiconductive behavior found at 1.25 nm could have an important impact on the scaling of the anomalous Hall effect.

With the electronic transport measurements, the longitudinal and Hall resistivities (ρ_{xx} and ρ_{xy}, respectively) were measured as a function of temperature and magnetic field (H). As we know, $\rho_{xy} = R_0 H + R_S M$,[12-15] we then define the anomalous Hall resistivity as $\rho_{AH} \equiv \rho_{xy} - R_0 H$. To further investigate the transport properties of Fe films thinner than 1.25 nm, the ρ_{AH} vs. ρ_{xx}^2 curve for Fe films was deduced, as shown in Fig. 3. The new scaling: $\rho_{AH} = (\alpha\rho_{xx0} + \beta\rho_{xx0}^2) + b\rho_{xx}^2$ proposed by Yuan Tian et al.[1] has been used to fit the data. This scaling fits the data very well with thickness between 1.79 nm and 17.04 nm, which means the skew scattering contributed from phonon scattering is negligibly small for the anomalous Hall resistivity.[9, 16-20] However, as film thickness went to 1.25 nm, an obvious departure at high temperature appears, as shown in Fig. 3**e-i**, especially in the thin film limit where the scaling model deviates the most. This is most due to the fact that the magnetization (M) drops quickly as the temperature approaching to the Curie temperature, since $\rho_{AH} = 4\pi R_S \times M$.[21, 22] However, we can still extract the intrinsic AHC coefficient b. We first assume M is constant at $T \leq T_c$. Then we can fit $\rho_{AH} = (\alpha\rho_{xx0} + \beta\rho_{xx0}^2) + b\rho_{xx}^2$ linearly at relatively low temperatures and retrieve the constant $\gamma(\gamma = \alpha\rho_{xx0} + \beta\rho_{xx0}^2)$ and b, as indicated by the solid lines in Fig. 3**e-i**. At relatively high temperatures, the magnetization then can be estimated as $M \sim \rho_{AH}/(\gamma + b\rho_{xx}^2)$, as shown in Fig. S3**c** and S3**d**. From this, we can estimate the Curie temperature by the equation $M = M_0 \times (1 - \frac{T}{T_c})^{\frac{1}{3}}$ (Fig. S4**a-b**).

The relationship between σ_{AH} and σ_{xx}^2 was plotted in Fig. 4**a-c**, for the equation can be written as $\sigma_{AH} = -(\alpha\sigma_{xx0}^{-1} + \beta\sigma_{xx0}^{-2})\sigma_{xx}^2 - b$, where $\sigma_{xx0} = 1/\rho_{xx0}$ is the residual conductivity. In the limit of $\rho_{AH} \ll \rho_{xx}$, we have the equation: $\rho_{AH} = -\sigma_{AH}\rho_{xx}^2$. Similar to the plot of ρ_{AH} versus ρ_{xx}^2, a linear relationship happens between σ_{AH} and σ_{xx}^2 at low temperature. However, for the relative high temperature, an obvious departure happens because of the decrease of M, shown in Fig. 4**a-c**.

Then we try to separate out the intrinsic Karplus-Luttinger (b term) from the side-jump as well as the skew-scattering contributions. The intrinsic term of Fe films with different thickness was obtained by linear fitting of ρ_{AH} versus ρ_{xx}^2 at low temperature, as shown in Fig. 4**d**. The intrinsic b term shows a decrease when the film thickness decreasing, which is similar to the result of others.[23] This b term was verified to come from the Karplus-Luttinger intrinsic contribution, which originated from the electronic band structure of the material. When the Fe film thickness is thicker than 1.25 nm, the Berry curvature contribution term (b)

in Fe reaches its bulk value. However, as the thickness approach 1.25 nm, the Berry curvature from the bulk begins to fade, which causes the decrease of the intrinsic b term.

In summary, we have studied the magnetic and electronic properties of high quality single crystal Fe films epitaxially grown on GaAs(100) at room temperature. We have observed a metal-semiconductor transition in the transport measurements, which originates from the thermally activated tunneling between metallic clusters. By using linear fitting of ρ_{AH} versus ρ_{xx}^2, we found that because of the magnetization decreasing, the role of this item shouldn't be ignored in the scaling of anomalous Hall effect for ultra-thin film. Furthermore, the intrinsic b term was found to drop when the film thickness decrease below 1.25 nm, which is related to the fading of the Berry curvature. This finding suggests us a more comprehensive understanding of the AHE, especially in the ultra-thin film limit, which is important for the development of spin-transistors for both data storage and process.

Acknowledgement

This work is supported by the State Key Program for Basic Research of China (Grants No. 2014CB921101), NSFC (Grants No. 61474061, 61274102 and 61427812), Jiangsu NSF (BK20140054), 'Jiangsu Shuangchuang Team' Program.

Reference

1. Tian, Y.; Ye, L.; Jin, X. *Physical Review Letters* **2009,** 103, (8).
2. Prinz, G. A. *Science* **1998,** 282, (5394), 1660-1663.
3. Wolf, S. A.; Awschalom, D. D.; Buhrman, R. A.; Daughton, J. M.; Von Molnar, S.; Roukes, M. L.; Chtchelkanova, A. Y.; Treger, D. M. *Science* **2001,** 294, (5546), 1488-1495.
4. Soda, T.; Minakawa, S.; Ohtake, M.; Futamoto, M.; Inaba, N. *Magnetics, IEEE Transactions on* **2015,** 51, (1), 1-4.
5. Minakawa, S.; Ohtake, M.; Futamoto, M.; Kirino, F.; Inaba, N. *J Appl Phys* **2015,** 117, (17), 17A903.
6. Florczak, J. M.; Dahlberg, E. D. *Physical Review B* **1991,** 44, (17), 9338-9347.
7. Wu, L.; Li, Y. F.; Xu, J. L.; Hou, D. Z.; Jin, X. F. *Physical Review B* **2013,** 87, (15).
8. Yao, Y. G.; Kleinman, L.; MacDonald, A. H.; Sinova, J.; Jungwirth, T.; Wang, D. S.; Wang, E. G.; Niu, Q. *Physical Review Letters* **2004,** 92, (3).
9. Jungwirth, T.; Niu, Q.; MacDonald, A. *Physical review letters* **2002,** 88, (20), 207208.
10. Filipe, A.; Schuhl, A.; Galtier, P. *Appl Phys Lett* **1997,** 70, (1), 129-131.
11. Xu, Y. B.; Kernohan, E. T. M.; Freeland, D. J.; Ercole, A.; Tselepi, M.; Bland, J. A. C. *Physical Review B* **1998,** 58, (2), 890-896.
12. Hall, E. H. *Phys Rev* **1900,** 10, (5), 277-310.
13. Crépieux, A.; Bruno, P. *Physical Review B* **2001,** 64, (1), 014416.
14. Berger, L. *Physical Review B* **1970,** 2, (11), 4559.
15. Nagaosa, N.; Sinova, J.; Onoda, S.; MacDonald, A.; Ong, N. *Reviews of modern physics* **2010,** 82, (2), 1539.
16. Crepieux, A.; Bruno, P. *Physical Review B* **2001,** 64, (1).
17. Bergmann, G.; Ye, F. *Physical Review Letters* **1991,** 67, (6), 735-738.
18. Dugaev, V. K.; Crépieux, A.; Bruno, P. *Physical Review B* **2001,** 64, (10).

19. Kotzler, J.; Gil, W. *Physical Review B* **2005,** 72, (6).

20. Mitra, P.; Misra, R.; Hebard, A. F.; Muttalib, K. A.; Wölfle, P. *Physical Review Letters* **2007,** 99, (4).

21. Zeng, C. G.; Yao, Y. G.; Niu, Q.; Weitering, H. H. *Physical Review Letters* **2006,** 96, (3).

22. Onoda, M.; Nagaosa, N. *Journal of the Physical Society of Japan* **2002,** 71, (1), 19-22.

23. Wu, L.; Zhu, K.; Yue, D.; Tian, Y.; Jin, X. *Physical Review B* **2016,** 93, (21).

Figures

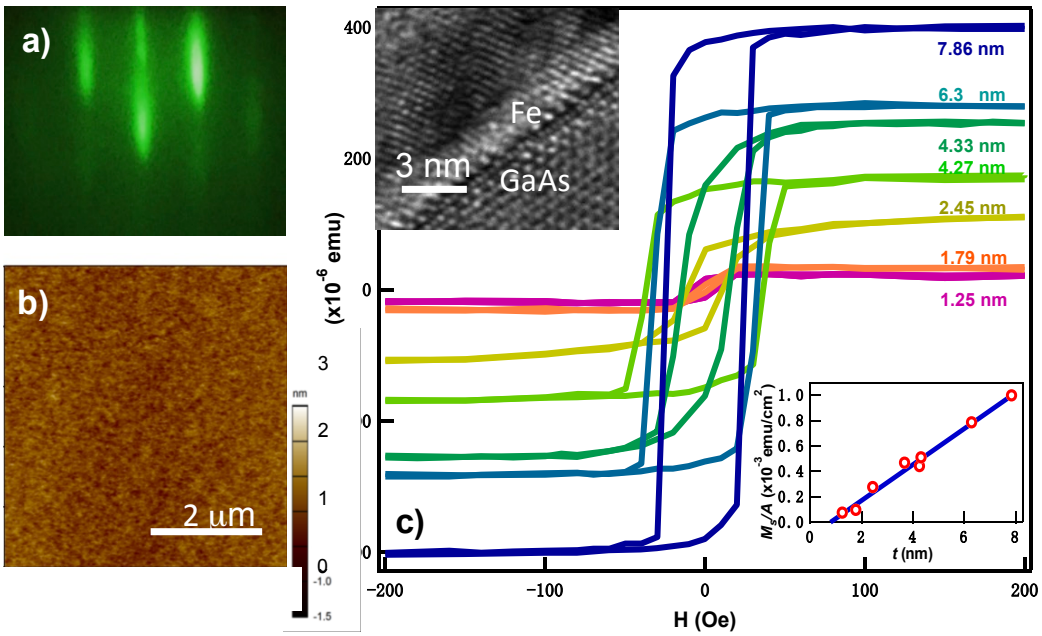

FIG. 1 **RHEED, AFM and VSM measurements of the Fe films.** (a) Streaky RHEED pattern of an as-grown Fe film with a thickness of 9.1 nm suggests 2D epitaxy growth. (b) Large area AFM topology of an Fe film, RMS = 0.16 nm. (c) Magnetization hysteresis loops for different Fe film thicknesses at room temperature. Top Inset: cross-sectional HRTEM image of 6.3 nm Fe/GaAs(100) hybrid structure. Bottom Inset: the thickness dependent saturation magnetization. The intercept of the linear fitting can be used to estimate the thickness of the dead layer: ~ 0.7 nm.

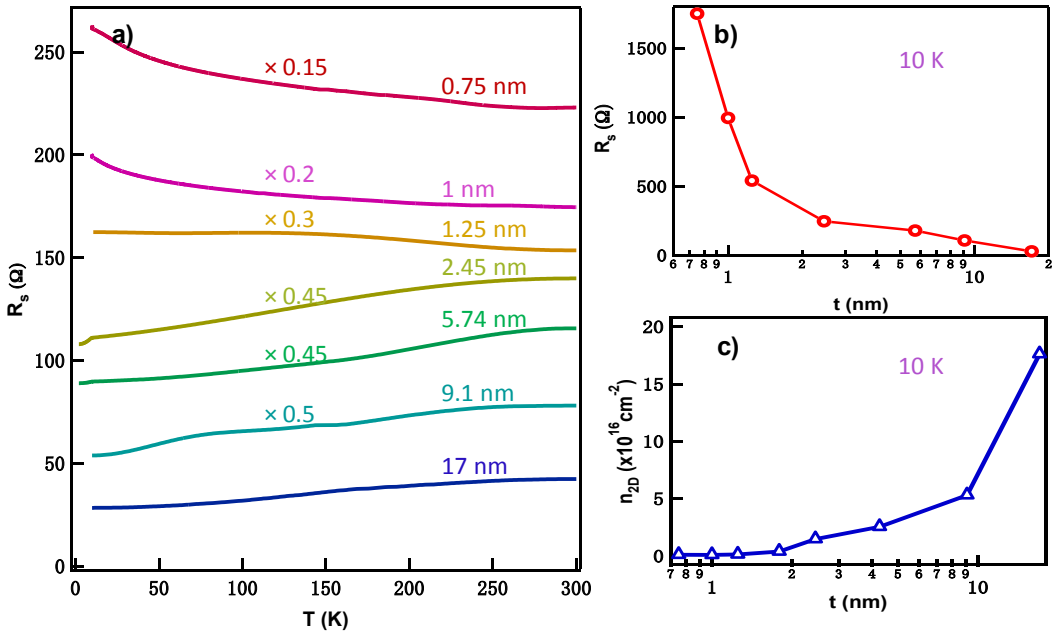

FIG. 2 ***R-T* and 2D carrier density characterization of Fe films**. (a) Temperature dependent sheet resistance (R_s) of the Fe films. As the thickness decreases from 17.04 nm to 0.75 nm, the films experience a metal-semiconductor transition at the critical thickness of 1.25 nm. (b) & (c) Sheet resistances and carrier densities at 10 K, demonstrate a monotonic dependence of the film thickness. There is a boom in R_s when film thickness decreases to 1.25 nm. Relatively, the carrier densities achieve a stable minimum for film thinner than the critical thickness.

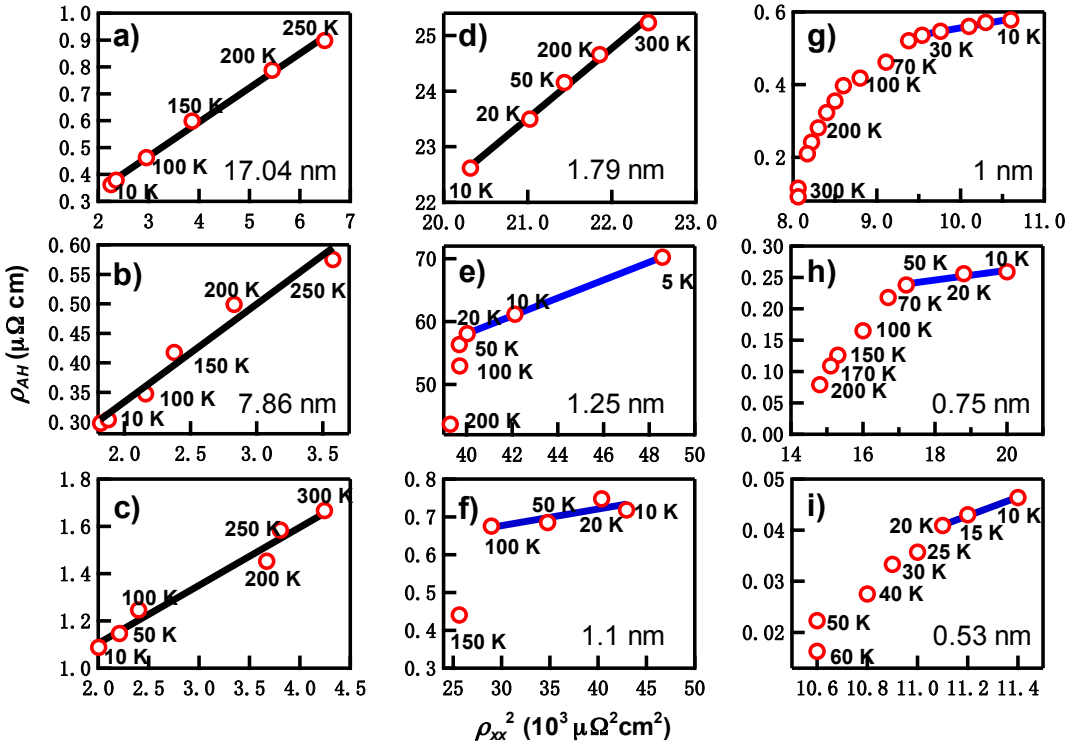

FIG. 3 **Linear fitting of ρ_{AH} versus ρ_{xx}^2.** (a)-(i) ρ_{AH} and ρ_{xx}^2 of films with various thickness. The solid black and blue lines are linear fitting results with $\rho_{AH} = \alpha\rho_{xx0} + \beta\rho_{xx0}^2 + b\rho_{xx}^2$. (a)-(d) when the film is thicker than 1.25 nm, the linear fitting suits all the temperature. (e)-(i) However, with thickness decreases, this linear fitting is only effective at low temperatures.

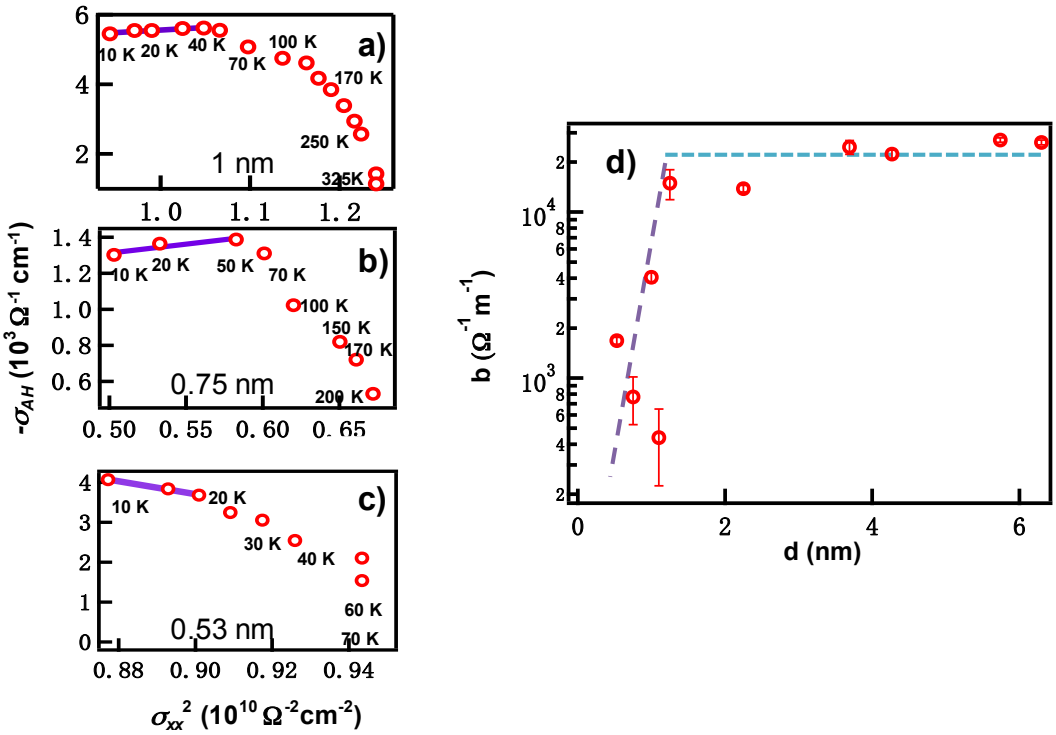

FIG. 4 **Linear fitting of $-\sigma_{AH}$ versus σ_{xx}^2**. (a)-(c) $-\sigma_{AH}$ and σ_{xx}^2 of films with various thickness, in which a similar reduction appears at high temperatures. (d) The thickness dependence of the intrinsic anomalous Hall conductivity coefficient b.